Astron. Astrophys. 353, 77–91 (2000)

ASTRONOMY AND ASTROPHYSICS

Evidence for the class of the most luminous quasars

II. Variability, polarization, and the gap in the M_V distribution

P. Teerikorpi

Tuorla Observatory, 21500 Piikkiö, Finland (pekkatee@deneb.astro.utu.fi)

Received 5 March 1999 / Accepted 3 November 1999

Abstract. We use 250 radio loud quasars with UBV photometry available and $z < 1.65$, to study whether there is a gap in the distribution of absolute magnitudes, from $M_V \approx -25.8$ (for $H_o = 100$ kms^{-1} Mpc^{-1}, q_o = 0.5) to -25.3, as was suggested by Teerikorpi (1981b; Paper I). In Paper I it was also proposed that there is a class of the most luminous radio quasars, differing in some properties from fainter quasars on the other side of the gap.

The main conclusion of Paper I remains intact. The gap in the distribution of absolute magnitudes is confirmed with the new formalism of cosmological Malmquist bias (Teerikorpi 1998), which allows one to use heterogeneous samples with magnitude inhomogeneity.

Comparison of optical variability and polarization of quasars on either side of the gap supports the conclusion in Paper I that the gap separates quasars with differing properties, with a tentative class "AI" around $M_V \approx -26.0$ (or -27.5 for $H_o = 50$). AI quasars are less variable than fainter quasars just beyond the gap, as already suggested in Paper I. Also, optical polarization of AI's is low, typically less than 1 percent, while beyond the gap one finds higher polarizations, mostly between 1 and 10 percent.

That the AI population is rare below $z \approx 0.5$ may relate to the observation that low-redshift quasars and radio galaxies avoid rich clusters. For $z < 0.5$ the variability of the fainter ones is similar to the AI with $z > 0.5$. For $z > 0.5$ the optical activity starts to increase. Optical polarization behaves in an analogous manner.

The evidence justifies further studies of the quasars in the AI absolute magnitude domain and its vicinity, including analysis of their radio properties and high resolution imaging of their hosts and environments at these intermediate redshifts (Papers III-IV). As the AI + the gap may be related to a phase of galaxy clustering, it is important to know at how high redshifts it is already present.

Key words: galaxies: quasars: general

1. Introduction

The present work bears on a permanent problem for active galactic nuclei (AGN): the absence of distinct subclasses among QSO's, in particular luminosity subclasses. If identified inside the wide luminosity range, they would give clues to the physics of the central engine and its relation to host galaxies and environment. They would illuminate the question of "luminosity vs. number density evolution" and suggest ways of testing the popular, though debated unified scheme. Luminosity classes of QSO's could also provide high-redshift "standard candles".

This study has its roots in Paper I (Teerikorpi 1981b) where a gap in the bright edge of the optical luminosity distribution of radio loud quasars was noted. Originally, the topic was galactic reddening (Teerikorpi 1981a: Paper Ia), for which evidence was sought from residuals $\delta(B-V)$ from the $(B-V)_o$ vs. z relation. The bright edge of the $\delta(B-V)$ vs. M'_V diagram (M'_V is the absolute magnitude corrected for the K-effect) was found to slope as expected for differential extinction, and *unexpectedly*, to be defined by a band of quasars. Hence, correcting M'_V along the reddening line resulted in a group of luminous quasars, apparently separated by a gap from the fainter ones.

Optical variability and some radio properties were inspected in Paper I for differences between the fainter quasars and the suggested separate group. These supported the idea of a subclass, though the data and methodology did not yet permit a definitive proof. New developments warrant a fresh look at this subject:

- The sample of UBV measured radio quasars has grown to about 250 ($z < 1.65$).
- There is more information on optical variations from monitoring programmes, and on optical polarization.
- The recent formalism of "cosmological Malmquist bias" (Teerikorpi 1998) may be applied to check the existence of the gap in the magnitude distribution.
- The large sample permits one to check the $(B-V)_o$ vs. z relation used in Paper I

Two points should be kept in mind when one looks especially at radio loud quasars. First, radio loud AGN's, including quasars and radio galaxies, are mostly hosted by elliptical galaxies (Wilson & Colbert 1995). Second, there is a strong selection difference between quasars and radio galaxies. One has access to optically luminous galaxies only. Quasars, with their higher luminosities, suffer less from this limitation at similar redshifts, and we sample a wider quasar, and plausibly, host galaxy lu-

minosity range. Hosts are not confined to giants (Bahcall et al. 1995) and there is evidence that luminosities of quasars and their hosts are correlated (Kotilainen et al. 1998). Though masked by quasar light, one may ask whether the hosts can leave a signature in the luminosity function (LF) of quasars, thus directing our attention to quasars with specific properties?

Consider, for instance, giant radio galaxies which define a narrow optical LF. The unified scheme says that such galaxies should harbour quasars. On the other hand, the masses of compact objects in the cores of galaxies are well correlated with the (bulge) mass of the host (Kormendy & Richstone 1995; Magorrian et al. 1998). After such information, it would not be so strange to find those quasars in a narrow luminosity range, perhaps separated by a gap from fainter quasars, hosted by other kinds of galaxies. Though just one possible scenario, it gives a reason to look carefully at the bright wing of quasars' LF which is also observationally best accessible.

It is also important to note that as the whole population of active galaxies has certainly evolved with look-back time, any distinct classes may exist only within restricted redshift ranges, corresponding to global evolutionary phases of the population.

The present paper studies the gap in the magnitude distribution, found in Paper I, and inspects optical properties of quasars on both sides of the gap (variability, polarization of light). Paper III will discuss properties of double radio sources, updating the analysis in Paper I, and Paper IV is planned to study host galaxies and cluster environments, based on observations at the subarcsecond resolution NOT telescope.

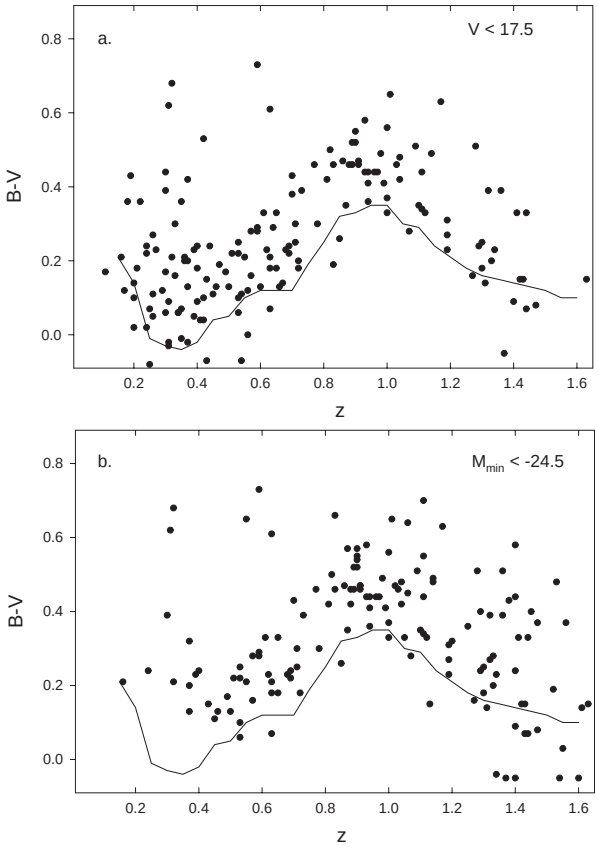

Fig. 1. a $B-V$ vs. z for quasars with $V_{cat} < 17.5$. **b** for the subsample with $M_{min} < -24.5$. The curve is the "zero-relation" adopted in Paper Ia.

2. The sample and optical data

The catalogs of Hewitt & Burbidge (1993) and Véron-Cetty & Véron (1993) were searched for data with criteria close to those in Paper Ia, i.e. $z < 1.65$, UBV photometry available, flux densities larger than 0.15 Jy at $\lambda = 11\ cm$. Now quasars with large optical variability are included in some parts of the analysis, though the study of the magnitude gap is made as in Paper I, i.e. excluding violent variables (amplitude > 1.2 mag). A new feature is that we can often replace the catalogue magnitude with a minimum brightness magnitude V_{min}.

The relevant area $z < 1.7, V < 17.5$ in the $z-V$ plane, is incompletely covered by UBV measured quasars. A well-defined magnitude-limited sample is needed for deriving a smoothed LF over a wide magnitude range (c.f. La Franca et al. 1994).

The present work has another aim within a narrow luminosity range, for which even the heterogeneous catalogs offer valuable data. First, we check with a larger sample whether the structure suggested by Paper I is still visible in histograms of absolute magnitudes, when one uses photoelectric magnitudes corrected for K-effect and extinction, and takes into account optical variability. Then, we verify whether the structure remains when one applies the method of cosmological Malmquist bias (Teerikorpi 1998). This will encourage us, in the third phase, to study whether the gap in the magnitude distribution separates quasars with different properties (this and Papers III-IV).

2.1. $B-V$ – reddenings. K_V – corrections

Paper Ia used quasars to study galactic extinction: discovered in radio, *luminous* quasars at medium redshifts are not easily pushed beyond the magnitude limit, when they happen to lie behind obscuring clouds. This very fact means that it is important to make extinction corrections to the magnitudes of radio selected quasars. A measure of extinction refering to the line of sight is optimal. Paper Ia concluded that the K-corrected $B-V$ colour is stable enough. The structure in the LF was noted only after $B-V$ was inspected as a reddening indicator.

Fig. 1a shows the $B-V$ vs. z diagram for $V < 17.5$ mag, and the $(B-V)_o(z)$ relation (shown as a line) from Paper Ia, approximating unreddened colours. This relation follows rather faithfully the lower envelope of the data. Hence, also the previous $K_V(z)$-terms, derived by Sandage's method from the $(B-V)_o(z)$ relation, are used here. In comparison, the K-terms of Cristiani & Vio (1990) differ at most 0.1 mag from these values[1].

[1] The zero point of reddening is roughly tied to A_B, the Galactic cosecant law coefficient. If one changes A_B, the $(B-V)_o(z)$ curve shifts up or down by $-0.3(A_B - 0.35)$. It is not critical here, which reasonable value of A_B is used. In Paper Ia it was concluded that $A_B \approx 0.35$ mag, and that $A_B > 0.2$ mag (at least).

Paper Ia and the Appendix A discuss $B-V$ as a reddening indicator. Above $z \approx 1.6$ the increased scatter in $B-V$ detoriates its use. In Paper Ia, the increase was partly ascribed to the emission line CIV (1549 Å) entering the B-band. Plausibly, the scatter is also due to the UV bump (Malkan 1983) and increased continuum variability at short wavelengths.

One might worry about the Baldwin effect: emission line strengths depend on continuum luminosity, causing scatter in $(B-V)_o$. However, in our restricted magnitude range, only a small systematic influence is expected. We show in Fig. 1b $B-V$ versus z below $M_{min} = -24.5$ mag: this important subsample defines a good zero-line especially in the range $0.5 < z < 1.3$ that will be shown to reveal best the proposed structure in the LF. Note that for $z < 0.5$, $B-V$ for luminous quasars deviates upwards from the "standard" relation based on all quasars.

2.2. Basic data

Table C1 in the Appendix C gives for the sample quasars the relevant data: z, absolute magnitude M_{min}, catalog magnitude V_{cat}, $B-V$, variability amplitude Δm, variability information level, and minimum flux magnitude V_{min}.

After Grandi & Tifft's (1974) list of optical amplitudes, used in Paper I, monitoring programmes have expanded the variability data. We collected such information using references in Grandi & Tifft (1974) and from more recent monitoring papers Scott et al. (1976), Pica et al. (1980), Moore & Stockman (1984), Lloyd (1984), Webb et al. (1988), and Smith et al. (1993). This search resulted in about 120 objects with the level of data given roughly as: 1 - notes on variability, 2 - monitoring < 2 years, 3 - monitoring > 2 years. Historical light curves (before 1950) were not considered.

With variability data, one may often replace the catalog magnitude V_{cat} by a minimum flux V_{min} that hopefully approaches a quiescent level of the quasar. From the data we derived the amplitude $\Delta m = m_{min} - m_{max}$. When possible, V_{min} was taken from the light curve. These are often in B or m_{pg}, requiring $B-V$, which adds uncertainty to V_{min}, but the error is less than typical variations. In some cases, noted in Table C1 as "4!", V is much fainter than the light curve level.

M_{min} is calculated from V_{min} with $q_o = 0.5$ and $H_o = 100$ $kms^{-1}Mpc^{-1}$, and it is corrected for the K-effect and extinction as in Paper Ia.

Much of the new photometry comes from a small telescope (Adam 1985), increasing errors in $B-V$ for faint objects. Even many bright ones have one old UBV observation only. In Table C1 interested observers find easily such cases. This paper also gives motivation for accurate photometry of bright quasars with no previous UBV.

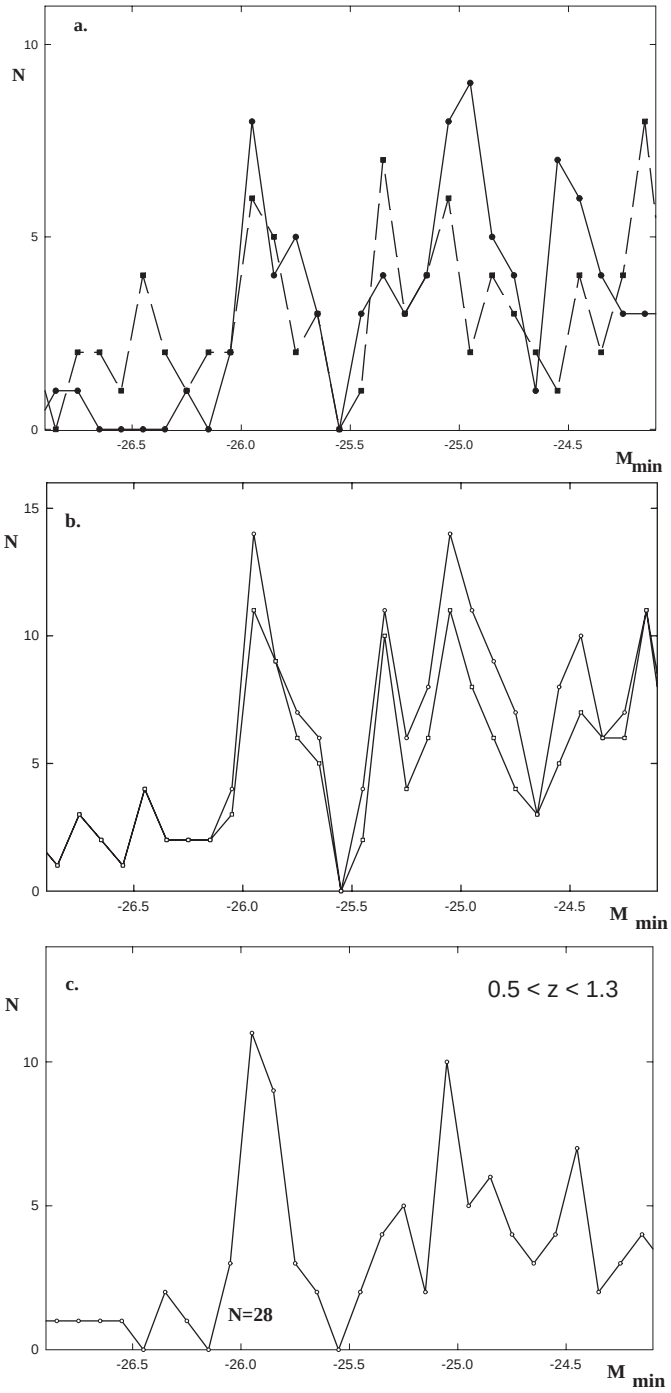

Fig. 2a–c. Distribution of M_{min}: **a** when variability information level is 1 – 3 (continuous curve) and without information, i.e. M_{cat} (dashed curve), **b** for all the quasars (upper curve) and for the quasars with a photoelectric V, **c** for quasars in the range $0.5 < z < 1.30$ and omitting objects with variability amplitude ≥ 1.2 mag. Now the AI peak contains 28 quasars.

3. Raw distribution of absolute magnitudes M_{min}

In Paper I we simply calculated the histogram of absolute magnitudes from the catalog apparent V_{cat} magnitudes of the sample quasars, corrected for the K-effect and Galactic extinction. With the Friedmann model parameters $H_o = 100$ and $q_o = 1$ the histogram suggested a peak at $M_V = -25.5$ and a gap around -25.2. Naturally, such a procedure does not produce any actual LF. At any redshift the magnitude limit cuts away quasars fainter than some absolute magnitude which depends on z. Generally,

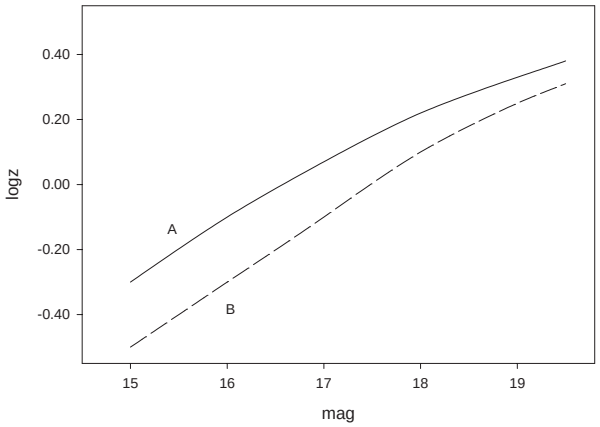

Fig. 3. A schematic display of the run of average $\log z$'s for two standard candles classes with different average absolute magnitudes and dispersions. Cosmological Malmquist bias makes the curves deviate from the standard Mattig curves, and they cannot be obtained from each other by a simple horizontal or vertical shift.

there is no unique magnitude limit and the incompleteness of the heterogeneous sample depends in an unknown manner on the magnitude and varies across the sky. The raw distribution of absolute magnitudes is strongly distorted (c.f. La Franca et al. 1994 showing that the general LF of radio quasars increases at least up to -23 mag). Nevertheless, we first inspect the histogram of absolute magnitudes, understanding that this may only give a noisy signal, if any, from a possible narrow LF structure.

In what follows, we use instead of $q_o = 1$ the more plausible value of $q_o = 1/2$ (without Λ; the present work does not discuss the Friedmann model parameters).

Repeating the calculation of Paper I with the *catalog* magnitudes of the present sample, we found that the feature at -25.5 was shifted to -26.0, and the gap is around -25.5. It is still our working hypothesis that this structure is due to a class separated by a gap from fainter quasars. The "hypothetical class" of Paper I, we call it now AI[2].

Fig. 2a shows the histograms of M_{min} and M_{cat}, for quasars with and without variability data, respectively. The AI feature is seen in both cases, though M_{cat} shows a tail of "overluminous" quasars and tend to scatter into the gap between AI and fainter quasars. This is as expected from variability.

The role of other than photoelectric (M_{min}) magnitudes is not large (recall that $B - V$ is needed for the reddening correction). A majority (60 percent) of M_{min} for the quasars with variability information come from a photoelectric V (i.e. V_{cat} is fainter than the estimated V from light curves or other source). Over 80 percent of all M_{min} come from a photoelectric V (see Fig. 2b).

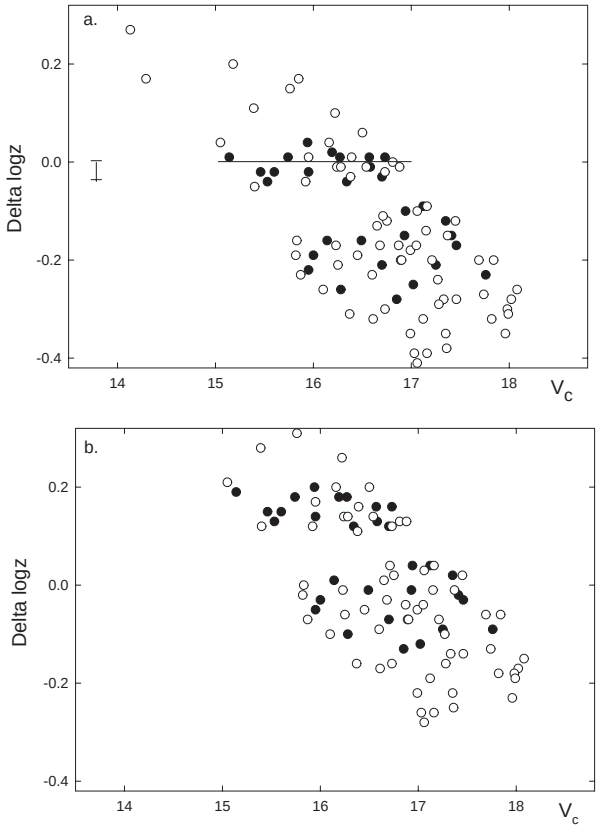

Fig. 4a and b. The difference $\Delta \log z$ between observed and predicted $logz$, when it is assumed that **a** $M_o = -26.0$ and $\sigma_M = 0.15$, and **b** $M_o = -25.2$ and $\sigma_M = 0.15$. The redshift range is $0.5 < z < 1.3$, and the objects with known variability ≥ 1.2 mag are not included. Filled/open circles denote quasars with/without variability information. In the upper panel the horizontal line at $\Delta \log z = 0$ indicates AI. The short vertical segment roughly indicates the influence of a 0.2 mag error in magnitude on the calculated redshift residual. The gap originally suggested in Paper I is now clearly visible.

A genuine AI feature should benefit from the exclusion of data that are known to increase scatter. Fig. 1b showed that the lower envelope of $B - V$ vs. z for luminous quasars is best defined when $0.5 < z < 1.3$. Restriction to this optimal z-range and excluding the most variable quasars (with amplitude ≥ 1.2 mag, as in Paper I), makes the putative peak stronger (Fig. 2c). Thus, even though noisy, the simple histograms motivate further study towards the 2nd phase, as outlined in the beginning of Sect. 2.

We emphasize that smoothed luminosity functions as derived e.g. by La Franca et al. (1994) for the study of the evolution of QSO populations, from a large complete sample, are not expected to reveal the structure here discussed. Variability, average extinction corrections, and wide redshift ranges will smooth out such details. Nevertheless, it is interesting to see from Fig. 5

[2] As noted by the referee, one may wonder if it is appropriate to use a bin of 0.1 mag, when the random error in the calculated M is at least as large, and when the suggested gap has a width of the same order. But the question is rather about the separation of a peak from the "edge" of the fainter quasar population. This separation would be about 0.5 mag. The point is how to define the position of a narrow peak, when random errors make it broader than in reality? One cannot use a bin which is much larger than the error. It should rather be smaller, because only in this way one can see the statistical (gaussian) envelope centered on the position of the peak. Naturally, a too small bin produces excessive noise and unreal features, which disappear when the size of the sample is increased.

of La Franca et al. (1994) that in the range $z < 1$ their LF of radio quasars practically ends around $M_V = -26.5$ (with our H_o), and in the range $1 < z < 2$, there is a steepening around -26.0.

4. The method of cosmological Malmquist bias

Calculating the histogram of absolute magnitudes is more or less equivalent to inspecting the Hubble diagram in the sense m vs. $logz$ and shifting the quasars along the standard Mattig (1958) curves down to the redshift corresponding to 10 pc in distance. As was noted above, such histograms do not display any true luminosity functions, and real structures such as gaps may be obscured by the complicated and unknown selection function of apparent magnitudes. Hence we use also another approach which abates these problems.

Teerikorpi (1998, hereafter T98) studied the influence of Malmquist bias on the run of Gaussian standard candles in the Hubble diagram ($\log z$ vs. m), i.e. the Malmquist bias of the 1st kind, in terms of Teerikorpi (1997). T98 showed that in the Friedmann universe one must replace the classical (constant) Malmquist bias correction by a cosmological correction which takes into account the differences from the ordinary r^3-volume and r^{-2} -flux laws and the non-zero K-effect.

The Malmquist bias in $\langle \log z \rangle$ comes to depend on the apparent magnitude m in a manner which depends on the average absolute magnitude M_o and the magnitude dispersion σ_M of the standard candle and also on the Friedmann model (H_o, q_o).

Such an understanding of what happens in the $\log z$ vs. m Hubble diagram has a useful application here: *it permits one to study the existence of standard candle-like subclasses and gaps between them when one has available only heterogeneous data.* It is sufficient to assume, reasonably, that at each apparent magnitude m the observed members of the subclass follow the underlying redshift (distance) distribution.

4.1. Schematic explanation

We illustrate the approach in Fig. 3, showing in a $\log z$ vs. m diagram two standard candle classes A and B with different average M_o and different σ_M. Now the *average* $\log z$'s do not follow the Mattig curves corresponding to (H_o,q_o,M_o). The expected run of $\langle \log z \rangle_m$ must be calculated from Eq. (13) of T98 where one replaces $m - f(z)$ by $m - f(z) - K(z)$. A subtlety was pointed out by T98: one should have in the $\log z$ vs. m diagram the apparent magnitude m *without* the K-correction (but with Galactic extinction correction) when one compares the data with the thus calculated theoretical predictions. Such a magnitude, corrected only for extinction, will be denoted by V_c. Then, the interesting quantity is the residual $\Delta \log z$

$$\Delta \log z = \log z - \langle \log z \rangle (V_c)$$

which for a genuine, non-evolving standard candle class should not vary as a function of V_c. This approach invites a few comments:

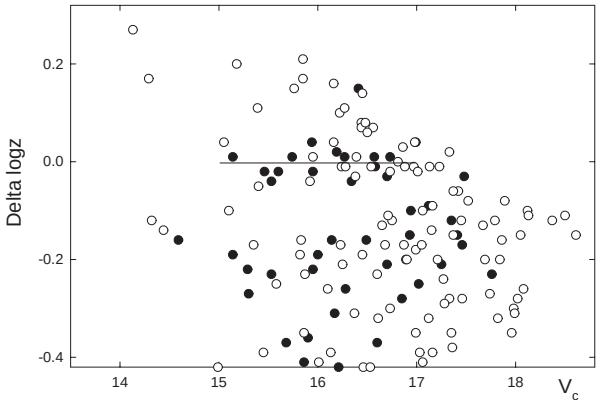

Fig. 5. The difference between observed and predicted $logz$, when it is assumed that $M_o = -26.0$ and $\sigma_M = 0.15$. The redshift range is now $0.1 < z < 1.65$.

Firstly, completeness variations in the apparent magnitude constitution of the sample do not affect the run of the $\log z$-residual and, in particular, the visibility of the real $\log z$ gap between A and B. *Secondly*, in general the width of the gap depends on V_c. *Thirdly*, though the detailed run of A and B depends on the cosmological model (and σ_M etc.), the gap is visible in the $\log z$-residuals even with an approximate model. *Fourthly*, there is an effect of optical variability: when the minimum magnitude is poorly or not known there will be a shift in $\langle \log z \rangle$ at a fixed V_c in comparison with the quasars for which m_{min} is better known. This should be taken into account in the calculation of the predicted $\langle \log z \rangle (V_c)$.

An estimate of the variability effect was obtained from the average difference $m_{min} - m_{cat}$ for the sample quasars with variability information level 2 or 3. For $M_{min} < -24.0$, this yields a difference of 0.2 mag which has been added to M_o in the calculation of $\langle \log z \rangle (V_c)$ for the quasars with poor or no variability information.

4.2. Application to the data and the reality of the gap

We present in Figs. 4 - 5 the $\Delta \log z$ vs. V_c diagram in three variants: for the z-range 0.5 - 1.3 where the predictions $\langle \log z \rangle (V_c)$ were calculated for $M_o = -26.0$ and -25.2 (Fig. 4), and for the total range 0.1 - 1.65, with $M_o = -26.0$ (Fig. 5). The deceleration parameter $q_o = \frac{1}{2}$. The dispersion σ_M is taken to be 0.15 mag in the displayed diagrams (other values from 0.0 to 0.3 were also tried, but the changes are not significant). The quasars with poor variability information, for which the magnitude shift of 0.2 was applied, are shown with a different symbol. The diagrams are restricted to quasars with $M_{min} < -24.0$ mag, hence the cut-off at small $\Delta \log z$. Note that the inclined right and left envelopes are caused by the redshift limits.

The small vertical bar approximately shows how much an error of 0.2 mag influences the calculated $\Delta \log z$-residual.

The diagrams reveal a clear gap over a wide apparent magnitude range in the distribution of the $\log z$ residuals, corresponding to the previously suspected gap in the distribution of absolute magnitudes, but now much more convincingly seen.

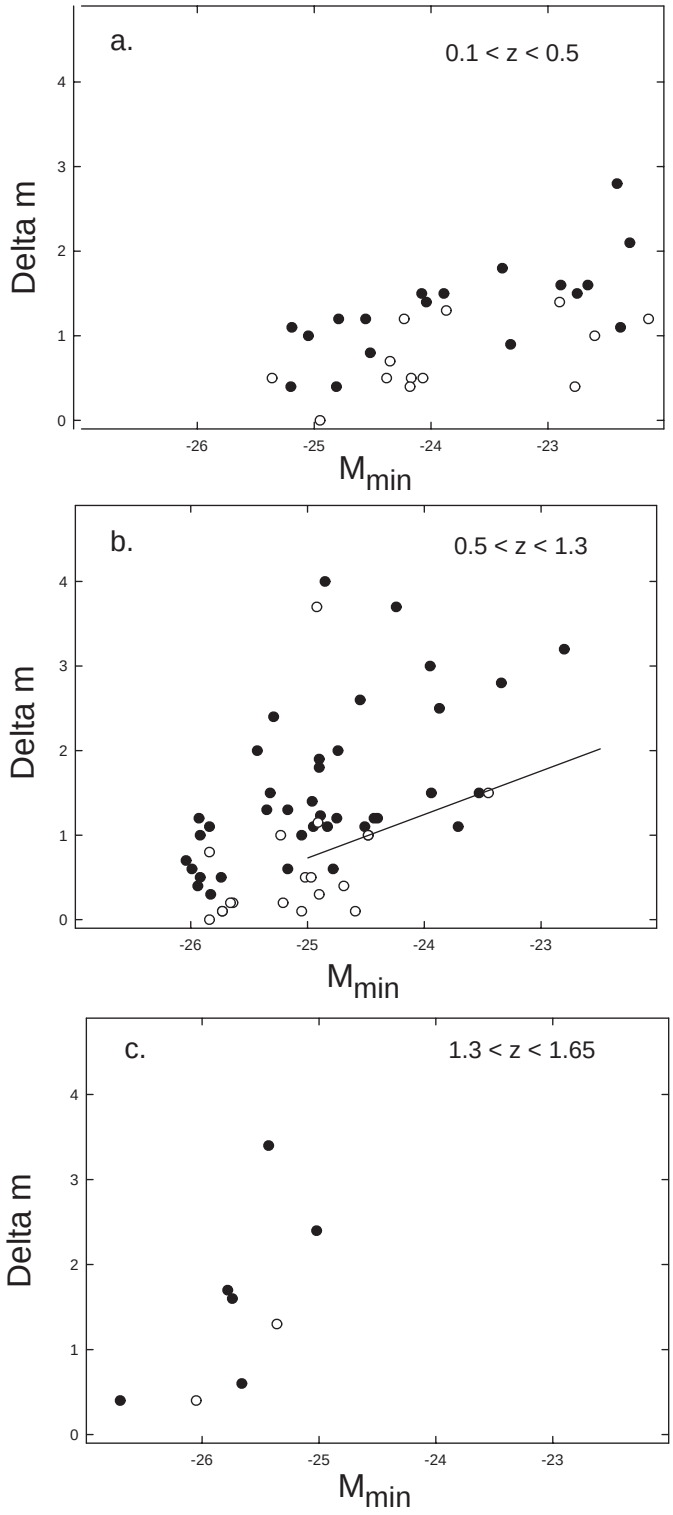

Fig. 6a–c. Variability amplitude against M_{min} for quasars with information level 2 (circle) or 3 (filled circle) in the redshift ranges **a** $0.1 < z < 0.5$, **b** $0.5 < z < 1.3$, **c** $1.3 < z < 1.65$. Increase of variability with decreasing luminosity and increasing redshift is contrary to what simple selection (apparent magnitude, slowing down by redshift) might produce. The line in **b** indicates the trend in the next smaller redshift range **a**.

This must be due to the present method which decreases the distortion in the M histograms caused by the heterogeneous magnitude selection.

4.3. Properties of the magnitude gap

The AI class, defined by the filled circles, appears as a horizontal concentration around $\Delta \log z \approx 0$, when $\langle \log z \rangle\ (V_c)$ is calculated with $M_o = -26.0$. The low- and high-z quasars added to Fig. 5 somewhat widen the apparent magnitude range where the gap is visible.

The gap gets narrower towards fainter magnitudes, because the lower edge of the gap steepens. The slope exists, though is smaller, even when one uses $M_o = -25.2$. This may reflect the simplified assumption that the lower edge can be treated as a standard candle. We have not considered any evolution. For example, if the comoving number density of quasars increases with redshift, it would make $\Delta \log z$ grow with V_c.

It is in general plausible that AI and the gap exist only in a restricted z-range, because of the evolution of the quasar population, e.g. via mergers of potential hosts in galaxy systems. Such questions, also related to the adopted Friedmann model, are outside of the scope of the present paper.

The steepening may also partly reflect unaccounted optical variability which shifts quasars over the magnitude limit towards brighter magnitudes and too small calculated $\langle \log z \rangle\ (V_c)$. Indeed, in Sect. 5 the "fainter edge" quasars are seen to be more variable than AI objects.

It is natural to ask whether the magnitude gap is a division line between objects of different properties, and specifically whether the class AI as was suggested in Paper I is a viable working hypothesis. Are there differences and in which properties when one crosses the gap between AI and the edge of the fainter LF part?

If they were to support the gap as a division line, the changes across the gap should not be just due to a gradual dependence on luminosity, and one would expect the contrast in some properties be large already close to the edge. We first inspect two interrelated optical characteristics: variability and polarization of light, for which quite some data exist.

5. Optical variability: dependence on luminosity

Paper I suggested that quasars in the AI range are less variable than fainter quasars. Indeed, for a visible structure to appear in the distribution of absolute magnitudes, such objects should not vary too much. Though amplitude Δm is not ideally defined (e.g. sampling periods and amounts of data vary from quasar to quasar), one wonders if the trend still exists when the sample is larger and variability better known.

Fig. 6 shows Δm vs. M_{min} for objects with monitoring level 2 or 3, in the z-ranges 0.1-0.5, 0.5-1.3, 1.3-1.65. Now also violently variable quasars are included. One sees the same thing as before: AI quasars are not very variable, and the optical activity increases when one crosses the gap. Note that this trend is best seen for well monitored quasars, as expected if it is real.

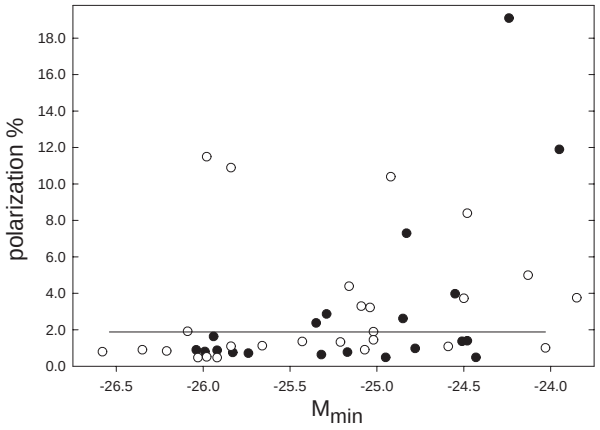

Fig. 7. Polarization against M_{min} for quasars in the redshift range $0.5 < z < 1.3$. Dots are quasars with good variability monitoring, open circle means poor or no variability information. Only polarization measurements with $P/\sigma_P > 2$ are included. The line indicates the level of 2 percent polarization. Typical error bars would be 0.3 - 0.4 percent.

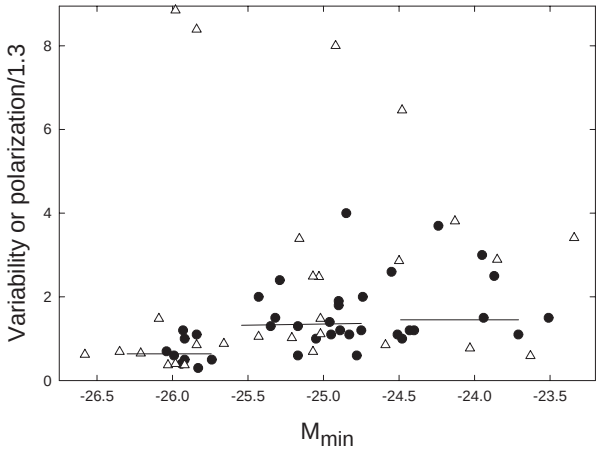

Fig. 8. Variability or polarization/1.3 against absolute magnitude M_{min} for AI quasars and for fainter quasars in the magnitude range -25.5 - -23.5. Redshift range is 0.5 - 1.3. Dots give variability from good monitoring, triangles give polarization/1.3, when good monitoring does not exist. The three horizontal line segments give medians for AI and the ranges -25.5 - -24.5 and -24.5 - -23.5.

Studies on how variability depends on luminosity or redshift have yielded varying conclusions (see Hook et al. 1994 and Véron & Hawkins 1995 for reviews). Most studies conclude that variability increases when luminosity decreases, both for radio loud and faint quasars. Generally the change has been taken as continuous, but interestingly, Véron & Hawkins (1995) noted for their sample of (mostly) radio faint QSO's an abrupt increase of variability around $M_B = -24.0$ (for $H_o = 100$, $q_o = 0$). Different sample criteria, corrections, and z ranges do not allow a direct comparison with the present result.

Fig. 6 shows that quasars with similar M vary above $z = 0.5$ more than at small redshifts (c.f. Fig. 8). Cristiani et al. (1996) also state that their optically selected sample is more active above $z = 1$, which may reflect the shift towards shorter rest wavelengths (Giallongo et al. 1991).

It is clear that AI is less variable than the fainter quasars in the z range 0.5 - 1.3 (at smaller z AI is absent). But is the difference significant already close to the edge beyond the magnitude gap? We used the median test (e.g. Mack 1975) to test the amplitude difference between AI and the fainter quasars, either down to $M_{min} = -24.8$ or -24.5, for well monitored quasars. The test tells that the difference is significant at better than 98 percent level for both cases. This agrees with the visual impression that the activity of well monitored quasars rather abruptly increases when the optical gap is crossed. Polarization gives further evidence, as discussed in the next section.

6. Optical polarization

Optical polarization and variability are connected. Highly polarized (> 2 percent) quasars typically are violently variable (Moore & Stockman 1984; Wills et al. 1992). In our sample, many quasars do not have good variability information, but have their polarization measured. Hence, one may complement Fig. 6 by polarization data. To this end, the major polarization lists were searched for data (Moore & Stockman 1984; Stockman et al. 1984; Impey & Tapia 1990; Berriman et al. 1990; Impey et al. 1991; Wills et al. 1992; Hutsemekers 1998). Only values with P/σ_P (polarization: error) larger than 2 were accepted, and when more than one measurement were reported, the best P/σ_P ratio was used. When polarization had clearly changed with time, the maximum value was taken. The raw polarizations in Table C1 were corrected for the error bias using the recipe of Simmons & Stewart (1985)[3].

These data show that all quasars with polarization higher than 2 percent, have optical variability (when known from good monitoring) larger than 1 mag. Fig. 7 shows the polarization against absolute magnitude for the quasars with (dots) and without (open circles) good monitoring. One notes the concentration of AI slightly below $P = 1$ percent (with two exceptions having very high polarizations > 10 percent; as they must be violently variable, their location on the AI part of the magnitude axis may well be accidental). Fainter quasars down to -24.5 have systematically higher polarization, with the median at 2 percent. Numbers are such that in AI magnitude range 2 out of 16 are highly polarized, while in the range -25.5 - -24.5 11 are highly and 11 low polarized.

Hence, the polarization of quasars, both with and without good variability monitoring, behaves as expected if their activity increases across the gap. Note that along the magnitude range of AI the small polarizations do not change, while they start to scatter over the 2 percent level when the magnitude gap is crossed.

Now we may combine variability (from good monitoring) and polarization (for quasars without good variability monitoring) in one diagram characterizing activity versus absolute magnitude in the redshift range 0.5 - 1.3 for AI and the M_{min} range

[3] The corrected polarization $P = \sqrt{(P_{obs}^2 - K^2\sigma^2)}$ where σ is the standard error of the observation and $K = 1.41$.

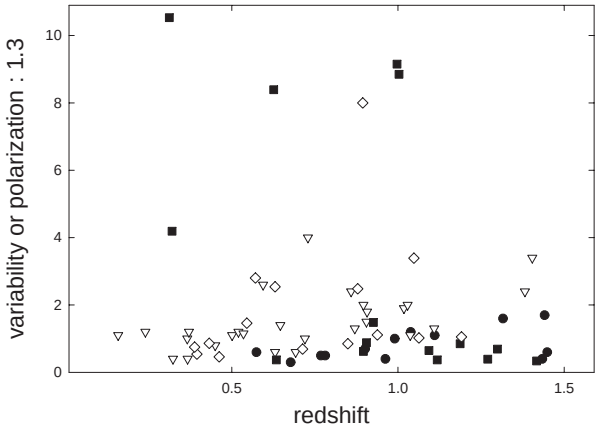

Fig. 9. Variability or polarization/1.3 against redshift z for AI quasars (filled symbols) and for fainter quasars in the magnitude range -25.5 - -24.5 (unfilled symbols). Circles and triangles give variability from good monitoring, squares and diamonds give polarization/1.3, when good monitoring does not exist.

down to -23.5. The diagram contains variability amplitude as such and polarization divided by 1.3 (such a factor conveniently normalizes AI's polarizations to equal their variability amplitudes, on the average).

Recalling that dots and triangles in Fig. 8 come independently from different quasars, the conclusion from Fig. 6b is still strengthened: there is a sudden significant change in activity, when the gap is crossed. Furthermore, the medians shown do not support that this change is just caused by a gradual increase of activity as a function of absolute magnitude in this redshift range.

Note also how AI is at all redshifts less active than the fainter quasars, and the increase of activity above $z \approx 0.5$ for the latter (Fig. 9).

7. Discussion

The gap in the distribution of absolute magnitudes of radio loud quasars has now been confirmed using a larger sample of quasars and implementing the $\log z$ vs. m (cosmological Malmquist bias) approach, and we can repeat the hypothesis/conclusion from Paper I: "... the envelope [in the Hubble diagram] is defined by a special class of the most luminous quasars ... separated by a gap from the fainter population". Though still fragmentary, this picture where the gap separates quasars with different properties forms a working hypothesis worth of further studies.

7.1. Central engine, host, environment

Narrow features in the luminosity distribution of quasars lead one to consider three necessary ingredients which according to the prevailing view determine the optical output of a quasar: the central engine (accretion onto a *supermassive compact object* MCO), with its mass M_{MCO} generally taken to be proportional to that of the *host galaxy*, and the cluster (or non-cluster) *environment*. What would a luminosity class within a wide redshift range from 0.5 up to at least 1.6 imply as regards these three factors and in which direction would it guide further investigations?

In Friedmann models such a z-range corresponds to a large fraction (about 30 percent) of the Hubble time. Contrary to individual galaxies shining over cosmological time-scales, quasars are generally regarded as short-lived phenomena (see e.g. Wisotzky 1998), though there is no exact knowledge of their lifetimes. Narrow features in the LF, such as AI or the gap, lead to the same conclusion.

It is thought that the luminosity of a quasar is directly proportional to the mass of the MCO. This mass doubles by accretion with the Eddington time-scale, about $4 \cdot 10^7$ yrs, if the quasar radiates at the Eddington limit. Hence a narrow LF structure would strongly hint at short-lived episodes powering the quasars. Furthermore, it suggests that the MCO's in question have similar masses, and hence, the host galaxies should form a class with a small dispersion in their masses (Kormendy & Richstone 1995; Magorrian et al. 1998)

7.2. Redshift range

The absence of AI below $z \approx 0.5$ (where fainter ones continue to be observed) may relate to the observation that low-redshift quasars and radio galaxies avoid rich clusters. Yee & Green (1987) and Fabian & Crawford (1990) connect this with changes in the clusters harbouring and fuelling luminous quasars. The potential central engines are still there, but the environment has changed. Another possibility is that there are quasar generations connected with different phases of mergers (Komberg 1982;1984).

Thus, if AI is linked to a dynamical phase of cluster evolution, ending around $z \approx 0.5$, it would be very interesting to know at how large redshifts AI population exists.

7.3. AI magnitude domain as a target of special study

The hypothesis that AI and the fainter quasars have systematically different central massive objects, host galaxies, or environments, makes one emphasize several lines of further studies.

1) The present results give motivation to gather more data on variability and polarization, reflecting the processes close to the MCO.
2) High resolution imaging of the hosts and environments around the AI magnitude domain in the redshift range 0.5 - 1.5 is needed in order to see if there are differences across the magnitude gap. Note that restriction to special objects where variability is known to be small, increases the host galaxy/quasar luminosity ratio, favouring the resolution of the host[4].

[4] A "blind" survey of the brightest quasars is biased towards smaller host/quasar ratios, because in addition to true "overluminous" objects, variability and gravitational lensing occasionally brighten even absolutely faint quasars. An imaging programme at the NOT is dedicated to the present problem (Paper IV).

3) Radio properties reflect both internal and environmental factors. In Paper I the asymmetry of double radio sources was found to change across the magnitude gap. This will be further studied in Paper III.
4) One should extend the study to higher redshifts. There photometry at longer wavelengths is needed in order to diminish the problems due to the K-correction, increased variability, and galactic extinction. If AI needs specific cluster environments, it is an indicator of the evolution of galaxy clusters.

8. Summary of conclusions

- New data support the existence of a gap in the absolute magnitude distribution of radio quasars, possibly separating a class or population AI of the most luminous quasars, at $M_V \approx -26.0$ (or -27.5 for $H_o = 50$), from fainter quasars. The gap in the bright end of the magnitude distribution is confirmed by the cosmological Malmquist bias approach.
- AI and the gap are seen especially well in the z-range $0.5 < z < 1.3$. The lower limit gives an epoch after which the number of AI quasars drops rapidly, while beyond $z \approx 1.3$ (especially 1.6) various problems start to affect the B and V bands, including increased variability. If AI is connected to a phase of galaxy clusters, it might exist within a restricted redshift range only.
- From AI to fainter objects, optical variability and polarization abruptly increase across the magnitude gap.
- AI's are less active, as measured by variability amplitude and polarization, than the fainter quasars at all redshifts where AI is observed.
- There is tentative evidence that the activity of both AI and the fainter population decreases towards the present epoch, and in case of AI may approach zero around $z \approx 0.5$ where AI become rare.
- Recent evidence for correlations between quasar and host galaxy luminosities, and between the masses of the compact central objects and the host galaxies, makes one expect that the hosts of a true AI class form a distinct class of galaxies, perhaps in a characteristic environment or dynamical state of the galaxy cluster. Thus they become important targets for deep, high-resolution imaging.

Acknowledgements. I thank Yu. Baryshev, B.V. Komberg, Chris Flynn, and the anonymous referee for useful comments. This study has been supported by the Academy of Finland (project "Cosmology in the local galaxy universe")

Appendix A: on reddening corrections

In Paper I and here, extinction corrections have been made using $B-V-(B-V)_o(z)$, multiplied by the total-to-differential extinction ratio R_V. The $B-V$ colour is preferred as a reddening indicator, because we believe that it gives a better estimate of the extinction along the line-of-sight than a measure averaged over several square degrees (galaxy counts or N_{HI}). For bright quasars, originally detected in the radio, the Holmberg-Fesenko selection (Teerikorpi 1978) works weaker, and one occasionally expects quite reddened quasars due to small scale extinction, unaccounted for by the smoothed-out measures. That such variations exist even at high galactic latitudes (Paper Ia), was directly shown by Hintz et al. (1997).

Also, the line-of-sight traverses dust in intervening galaxies. This is increasingly important at redshifts > 1, and is automatically included in the reddening. With a universal extinction law $\propto 1/\lambda$ (λ is the wavelength), in the extinction ratio R_V the dependences on the redshift of the dust cancel out, as shown in Appendix B.

It is difficult to get direct evidence on the accuracy of $E(B-V)$ under small scale extinction variations - in fact, the proof may come in an indirect way, e.g. that real features in the LF are revealed when magnitudes are individually corrected. Nevertheless, we below summarize results from the our programme of extinction studies at high galactic latitudes, supporting the use of $E(B-V)$.

• Paper Ia: $E(B-V)$ was shown to be correlated with N_{HI}: the standard reddening vs. neutral hydrogen relation appeared, together with an "upper branch" of higher reddenings in the direction of the Local Spiral Arm, interpreted as due to compact clouds within it. In the next paper it was related to high latitude molecular clouds.
• Haarala & Teerikorpi (1986): $E(B-V)$ estimates for close (< 3 deg) quasar pairs are correlated. There is an expected relation between $E(B-V)$ and $\log N$(Lick counts/deg^2).
• Teerikorpi & Kotilainen (1989) found a correlation between $E(B-V)$ and star/galaxy counts from the PSA prints, above $b = 50$ deg, with a $5' \times 5'$ resolution.
• Teerikorpi (1990): The enigma of the nearly zero reddenings for stars at high galactic latitudes, was explained by a Malmquist-like effect. The corrected reddenings approach at high northern vertical distances Z the values predicted by de Vaucouleurs's model ($A_B \approx 0.20$ mag). For quasars, the average extinction is larger, because compact dust clouds are better represented in a radio detected sample. Interstellar polarization for distant (up to 800 pc) high latitude stars has confirmed the increasing extinction (Berdyugin et al. 1995; Berdyugin & Teerikorpi 1997).

Appendix B: reddening, extinction and R_V for different absorber redshifts

In Paper I the total-to-differential extinction ratio R_V was shown to vary little with quasar redshift for typical quasar spectra, if the dust is in our Galaxy (at zero redshift), and has the average value of about 3.3. If the dust lies at some redshift z between the quasar and us, one again does not expect a large influence on R_V, though same amounts of dust at different z will cause significantly different effects on the light received at $z = 0$ (Ostriker & Heisler (1984). Here we show how the idealized extinction curve $\propto 1/\lambda$ leads to particularly simple results.

The normalized interstellar extinction curve is written as (e.g. Savage & Mathis 1979):

$$E(\lambda - V)/E(B-V) = A(\lambda)/E(B-V) - R_V$$

Table C.1. Basic sample ($M_{min} < -22.0$ mag)

RA	δ	z	M_{min}	V_{cat}	$B-V$	Δm	var	V_{min}	note	ref	P	σ_P	P-ref
0003	+1553	0.450	-24.52	16.40	0.11	0.8	3	16.40		42	0.62	0.16	S84
0003	- 0021	1.037	-23.51	19.35	0.79	1.5	2	20.30	2	39			
0005	-2356	1.410	-27.21	16.47	0.33	-.-	0	16.47					
0024	+2225	1.118	- 26.03	16.57	0.33	-.-	0	16.57			0.63	0.29	S84
0029	-4124	0.896	-24.99	17.82	0.57	-.-	0	17.82					
0036	-3916	0.592	-26.90	16.29	0.73	0.0	1	16.29	1	1,2			
0047	-8313	1.112	-26.20	17.53	0.70	1.5	1	17.53		2,23			
0056	-0009	0.717	-24.40	17.33	0.20	1.2	3	17.33	4	42			
0100	+0954	0.465	-22.58	18.18	0.02	-.-	0	18.18					
0122	-0021	1.070	-25.64	16.70	0.28	0.2	2	16.70		2,7	0.45	0.57	S84
0122	-0416	0.561	-24.05	17.03	0.00	-.-	0	17.03					
0125	-4128	1.099	-25.32	17.25	0.35	-.-	0	17.25					
0130	-1710	1.020	-24.23	18.44	0.46	-.-	0	18.44					
0133	+2042	0.425	-22.41	18.10	0.05	2.8	3	18.32	4	9,33	1.62	0.36	MS84
0134	+3254	0.367	-25.20	16.20	0.42	0.4	3	16.29	1	25,38	1.8	0.2	S84,IT90
0135	-2446	0.831	-24.47	17.33	0.19	-.-	0	17.33			0.6	1.0	IT90
0135	-0542	0.308	-22.00	18.25	0.04	0.4	2	18.25		34,19			
0137	+0116	0.260	-22.77	17.07	0.05	0.4	2	17.07		34,19			
0137	-0105	0.334	-22.90	16.49	-.12	1.4	2	17.27		30	0.63	0.31	S84
0155	-1058	0.616	-24.53	17.09	0.23	-.-	0	17.09					
0159	-1147	0.669	-24.43	16.40	0.14	1.2	3	17.05	2	42	0.65	0.30	S84
0202	-7634	0.389	-23.79	16.90	0.05	-.-	0	16.90					
0208	-5115	1.003	-25.98	16.93	0.56	-.-	0	16.93			11.5	0.4	IT90
0232	-0415	1.434	-26.70	16.46	0.15	0.4	3	16.46		20,33	0.91	0.32	S84
0306	+1017	0.863	-23.93	18.40	0.45	-.-	1	18.40					
0336	-0156	0.852	-24.24	18.41	0.55	3.7	3	18.41	4!	42	19.4	2.4	IT90
0340	+0448	0.357	-22.38	19.17	0.35	1.1	3	19.17		37			
0349	-1438	0.614	-25.73	16.22	0.33	0.1	2	16.22		33	0.55	0.37	S84
0350	-0719	0.962	-25.94	16.49	0.44	0.4	3	16.49		33	1.67	0.24	S84
0355	-4820	1.005	-25.84	16.38	0.33	-.-	0	16.38					
0402	-3613	1.417	-25.95	17.17	0.15	-.-	0	17.17			0.60	0.30	IT90
0403	-1316	0.571	-24.50	17.17	0.28	0.8	1	17.17		10	3.80	0.50	IT90
0405	-1219	0.574	-25.99	14.82	0.16	0.6	3	15.30	1,2	3,43,2,32	0.83	0.16	S84
0414	-0601	0.781	-25.74	15.94	0.30	0.5	3	16.20	2	37	0.78	0.22	S84
0420	-0127	0.915	-23.95	17.76	0.58	3.0	3	18.90	2	42	11.9	0.5	IT90
0422	-3803	0.782	-23.51	18.18	0.07	-.-	0	18.18					
0439	-4319	0.593	-25.36	16.36	0.28	-.-	0	16.36					
0440	-0023	0.850	-22.80	19.22	0.37	3.2	3	19.22	4	42	2.7	1.6	IT90
0448	-3916	1.288	-26.61	16.46	0.24	-.-	0	16.46					
0454	+0356	1.345	-26.66	16.53	0.23	-.-	0	16.53			0.32	0.28	S84
0454	-2204	0.534	-24.89	16.10	0.06	1.1	3	16.10	4	42	0.37	0.29	W92
0506	-6113	1.093	-26.21	16.85	0.51	-.-	0	16.85			1.1	0.5	IT90
0514	-1606	1.278	-26.96	16.95	0.51	-.-	0	16.95					
0518	+1635	0.759	-23.94	18.84	0.53	1.5	3	18.84		28	2.2	2.2	IT90
0522	-6110	1.400	-24.99	18.05	-.05	-.-	0	18.05					
0537	-4406	0.894	-24.92	15.47	0.46	3.7	2	17.50	3	1,14,35	10.4	0.5	IT90
0538	+4949	0.545	-25.02	17.80	0.65	0.5	2	17.80		19,34	2.3	0.9	IT90,I91,W92
0621	-7841	0.942	-25.34	16.96	0.41	-.-	0	16.96					
0622	-4411	0.688	-24.87	16.93	0.22	-.-	0	16.93					
0637	-7513	0.651	-26.32	15.75	0.33	-.-	0	15.75			0.3	0.2	IT90
0709	+3701	0.487	-25.75	15.49	0.17	-.-	0	15.49					
0710	+1151	0.768	-25.92	16.60	0.46	0.5	3	16.60		25	0.10	0.27	S84
0725	+1443	1.382	-25.02	18.92	0.43	2.4	3	18.92	4	42			
0736	+0143	0.191	-23.32	16.47	0.43	0.9	3	16.47		42	1.1	0.4	IT90
0738	+3119	0.630	-25.17	16.14	0.07	0.6	3	16.14	2	42	0.44	0.39	S84,W92
0740	+3800	1.063	-25.21	17.60	0.45	0.2	2	17.60		34	1.65	0.69	W92
0742	+3150	0.462	-25.40	15.63	0.13	-.-	0	15.63			0.64	0.16	S84

Table C.1. (continued)

RA	δ	z	M_{min}	V_{cat}	$B-V$	Δm	var	V_{min}	note	ref	P	σ_P	P-ref
0743	-6719	0.395	-24.95	16.37	0.24	0.0	2	16.37		2,18	0.9	0.4	IT90
0809	+4822	0.871	-24.97	17.79	0.57	0.5	2	17.79		19,34	0.7	0.6	IT90,I91
0812	+0204	0.402	-24.04	17.10	0.18	1.4	3	17.10	4	42			
0827	+2421	0.939	-24.86	17.26	0.36	-.-	0	17.26					
0827	+3752	0.914	-24.20	18.11	0.42	-.-	0	18.11					
0833	+6524	1.112	-25.05	18.21	0.55	0.1	2	18.21		34			
0835	+5804	1.534	-26.78	17.62	0.48	-.-	0	17.62					
0838	+1323	0.684	-24.34	18.15	0.43	0.7	1	18.15		45			
0839	+1846	0.259	-24.19	16.36	0.27	-.-	0	16.36			1.74	0.53	W92
0850	+1403	1.109	-25.17	17.42	0.34	1.3	3	17.42		42	1.05	0.50	MS84
0855	+1421	1.048	-25.16	19.06	0.90	-.-	0	19.06			5.31	2.12	MS84
0856	+1703	1.449	-25.66	17.90	0.40	0.6	3	18.34	2	45,46,26			
0858	-7707	0.490	-23.77	17.57	0.20	-.-	0	17.57					
0859	-1403	1.335	-26.48	16.59	0.20	-.-	0	16.59			1.07	0.65	S84,W92
0903	+1658	0.411	-22.14	18.27	0.21	1.2	2	19.10	2	46			
0906	+0133	1.018	-24.90	17.79	0.47	1.9	3	17.79	2	2,42,47			
0906	+4305	0.670	-23.85	18.48	0.49	0.5	1	18.80		24	3.80	0.40	IT90
0911	+0520	0.303	-23.21	17.43	0.17	0.1	1	17.43		45			
0922	+1457	0.896	-24.74	17.96	0.54	2.0	3	17.96	4	42			
0923	+3915	0.699	-23.63	17.86	0.06	1.3	1	17.86		33	0.91	0.35	MS84
0925	-2021	0.348	-24.20	16.40	0.07	-.-	0	16.40					
0932	+0217	0.659	-24.04	17.39	0.13	-.-	0	17.39					
0952	+1757	1.472	-25.94	17.23	0.08	-.-	0	17.23					
0952	+0944	0.298	-23.00	17.24	0.06	0.2	1	17.24		45			
0953	+2529	0.712	-24.51	17.21	0.25	1.1	3	17.40	2	42	1.45	0.33	W92
0955	+3238	0.530	-24.75	15.78	0.10	1.2	3	16.30	2	19,25	0.18	0.24	S84
0957	+0019	0.907	-24.90	17.57	0.47	1.8	3	17.57	4	42			
1004	-0152	1.212	-23.78	19.24	0.32	-.-	0	19.24					
1004	+1303	0.240	-24.56	15.15	0.24	1.2	3	15.60	1,2,4	12,42	0.79	0.11	S84
1004	-2144	0.330	-23.90	16.89	0.16	-.-	0	16.89					
1011	-2816	0.253	-22.69	16.88	-.08	-.-	0	16.88					
1018	+3452	1.404	-25.63	17.75	0.24	-.-	0	17.75					
1019	+3056	1.316	-25.74	17.51	0.27	1.6	3	17.51	4!	42			
1020	-1022	0.197	-22.85	16.11	0.14	-.-	0	16.11			0.58	0.24	S84
1022	+1927	0.828	-24.90	17.49	0.46	0.5	1	17.49		45			
1028	+3118	0.177	-22.62	16.71	0.36	-.-	0	16.71			0.25	0.23	S84
1034	-2918	0.312	-25.72	16.46	0.62	-.-	0	16.46			13.8	1.18	IT90,W92
1038	+0625	1.270	-25.98	16.81	0.16	0.2	1	16.81		45	0.62	0.24	S84
1040	+1219	1.029	-25.43	17.29	0.46	2.0	3	17.29	4!	42			
1046	+0521	1.115	-23.47	18.94	0.24	0.2	1	18.94		45			
1047	+0941	0.786	-24.42	17.86	0.40	0.7	1	17.86		45			
1048	-0902	0.344	-23.76	16.79	0.06	0.3	1	16.79		40	0.85	0.30	S84
1049	+6141	0.422	-23.89	16.48	0.10	1.5	3	17.00	2	29	0.83	0.34	S84
1050	-1829	0.544	-23.96	17.06	-.07	-.-	0	17.06					
1055	+2007	1.110	-25.84	17.07	0.44	1.1	3	17.07		36			
1055	-0434	1.428	-25.31	17.79	0.07	-.-	0	17.79					
1055	+0150	0.888	-24.13	18.28	0.46	1.6	1	18.28		21	5.0	0.5	IT90,W92
1057	+1005	1.317	-26.45	17.20	0.39	-.-	0	17.20					
1058	+1102	0.420	-22.60	17.10	0.04	1.0	2	18.10	3	26,45			
1100	+7715	0.311	-24.35	15.72	-.02	0.7	2	15.72		25	0.71	0.22	S84
1101	-3235	0.354	-24.07	16.30	-.01	0.5	2	16.30		18			
1103	-0036	0.426	-24.14	16.46	-.07	-.-	0	16.46			0.37	0.26	S84
1104	+1644	0.634	-25.92	15.70	0.21	0.0	1	15.70		45	0.56	0.21	S84,BT99
1111	+4053	0.734	-23.60	17.98	0.15	-.-	0	17.98					
1116	-4617	0.713	-25.07	17.00	0.30	-.-	0	17.00			1.0	0.3	IT90
1117	-2451	0.466	-24.17	17.07	0.19	0.5	2	17.07		1,2,18			
1127	-1432	1.187	-25.84	16.90	0.27	0.0	2	16.90		1,2,36,37,16	1.26	0.44	S84,W92

Table C.1. (continued)

RA	δ	z	M_{min}	V_{cat}	$B-V$	Δm	var	V_{min}	note	ref	P	σ_P	P-ref
1130	+1040	0.540	-23.58	17.49	0.11	0.0	1	17.49		1,2,45			
1132	+3022	0.614	-23.41	18.24	0.24	-.-	0	18.24					
1136	-1334	0.554	-25.23	16.17	0.21	-.-	0	16.17			0.3	0.2	IT90
1137	+6604	0.646	-24.96	16.32	0.18	1.4	3	16.60	2	4,5	0.35	0.20	S84
1146	-0347	0.341	-23.63	16.90	0.06	-.-	0	16.90			0.40	0.27	S84
1148	+3842	1.303	-25.89	17.04	0.18	-.-	0	17.04					
1150	+4947	0.334	-23.87	17.10	0.30	1.3	2	17.40	2	9	1.25	0.76	W92
1150	+0930	0.698	-24.14	17.58	0.19	-.-	0	17.58					
1153	+3144	1.557	-25.13	18.96	0.37	-.-	0	18.96					
1156	+2931	0.729	-24.85	14.41	0.39	4.0	3	17.50	2	42	2.68	0.41	W92
1158	+0044	1.370	-23.90	19.09	0.14	-.-	0	19.09					
1159	-0337	1.102	-23.33	19.41	0.40	-.-	0	19.41					
1203	+1059	1.088	-24.29	18.08	0.23	0.7	1	18.08		2,45			
1206	+4356	1.400	-26.05	18.42	0.58	0.4	2	18.42		34			
1206	-3959	0.966	-25.43	17.00	0.44	0.0	1	17.01	1	1,2			
1208	+3213	0.388	-24.58	16.68	0.23	0.3	1	16.68		31	1.03	0.24	S84
1210	+1324	1.137	-25.08	18.09	0.48	0.0	1	18.09		45			
1211	+3326	1.598	-25.38	17.89	-.05	-.-	0	17.89			0.91	0.49	S84
1215	+1121	1.396	-26.18	16.86	0.09	-.-	0	16.86			0.36	0.34	S84
1216	-0103	0.415	-24.47	15.64	0.53	2.0	1	17.80	3	13			
1217	+0220	0.240	-22.75	16.53	0.02	1.5	3	16.69	4	12,42	0.18	0.28	S84
1218	+3359	1.519	-24.86	18.61	0.19	0.0	1	18.61		34			
1219	+0429	0.965	-24.16	17.98	-.10	-.-	0	17.98					
1221	+1837	1.401	-24.44	18.74	0.18	0.5	1	18.74		45			
1222	+0347	0.957	-23.40	19.02	0.44	-.-	0	19.02					
1222	+2139	0.435	-23.26	17.50	0.06	-.-	0	17.50					
1223	+2515	0.268	-23.39	17.12	0.23	0.4	1	17.12		22	0.66	0.38	S84
1226	+0219	0.158	-25.19	12.86	0.21	1.1	3	13.30	2	42	0.21	0.04	S84
1229	-0207	1.038	-25.93	16.75	0.48	1.2	3	16.90	4	1,37	0.10	0.53	S84
1232	-2455	0.355	-24.38	17.20	0.36	0.5	2	17.20		2,18			
1237	-1007	0.753	-23.51	18.11	-.03	1.5	3	18.11	4	2,37			
1240	-2926	1.133	-24.76	17.69	0.15	-.-	0	17.69					
1241	+1639	0.557	-22.47	19.00	0.23	0.4	1	19.00		45			
1244	-2531	0.638	-24.48	17.41	0.29	1.0	2	17.41		2,18	8.40	0.20	IT90
1250	+5650	0.320	-22.16	17.93	-.17	-.-	0	17.93					
1252	+1157	0.870	-25.35	16.64	0.35	1.3	3	16.64	4	42	2.51	0.56	S84,W92
1253	-0531	0.536	-23.16	17.75	0.26	6.6	3	18.40	2	2,6,42,47	9.00	0.40	IT90
1258	+2846	0.645	-23.82	17.53	0.09	-.-	0	17.53					
1258	+2837	1.374	-23.59	19.40	0.05	-.-	0	19.40					
1302	-0329	1.250	-23.51	19.42	0.24	-.-	0	19.42					
1302	-1017	0.286	-24.23	14.92	0.12	1.2	2	16.10	2	11,33	0.41	0.31	S84,W92
1305	+0658	0.602	-24.23	17.02	0.13	-.-	0	17.02					
1306	+2724	1.537	-24.73	18.50	-.05	-.-	0	18.50					
1308	+3236	0.997	-27.03	15.24	0.37	-.-	0	15.24			12.10	1.50	IT90
1317	-0033	0.890	-25.30	17.32	0.52	-.-	0	17.32					
1327	-2126	0.528	-24.69	16.74	0.22	0.4	2	16.74		2,18			
1327	-2040	1.169	-26.77	17.04	0.63	-.-	0	17.04					
1328	+2524	1.055	-25.73	17.67	0.64	0.1	2	17.67		6,33,38	0.6	0.7	IT90,W92
1328	-2623	0.883	-24.67	17.59	0.42	-.-	0	17.59					
1328	+3045	0.849	-24.59	17.25	0.26	0.1	2	17.25		33,38	1.29	0.49	IT90,W92
1331	+0234	1.228	-23.83	18.85	0.19	-.-	0	18.85					
1335	+0222	1.356	-26.40	17.73	0.51	-.-	0	17.73					
1335	-0611	0.625	-23.68	17.68	0.14	-.-	0	17.68					
1340	+6036	0.961	-24.14	18.12	0.39	-.-	0	18.12					
1340	+2859	0.905	-25.32	17.07	0.47	1.5	3	17.15		31,24a	0.81	0.35	S84
1351	+2646	0.310	-22.85	17.18	-.03	-.-	0	17.18					
1354	+1933	0.720	-25.05	16.02	0.18	1.0	3	16.60	4	3,37	0.34	0.27	S84,W92

Table C.1. (continued)

RA	δ	z	M_{min}	V_{cat}	$B-V$	Δm	var	V_{min}	note	ref	P	σ_P	P-ref
1355	-4138	0.313	-24.18	15.86	-.10	0.4	2	15.86		2,18			
1356	+5806	1.371	-25.62	17.37	-.05	-.-	0	17.37			0.40	0.29	S84
1356	+0214	1.329	-25.05	18.27	0.28	-.-	0	18.27					
1415	+1717	0.821	-25.09	17.46	0.50	-.-	0	17.46			0.85	0.52	S84
1416	+0642	1.440	-26.96	16.79	0.33	-.-	0	16.79			0.77	0.39	S84
1416	+1554	1.472	-26.19	17.75	0.37	-.-	0	17.75			1.06	0.85	S84
1421	+1213	1.611	-25.36	18.04	0.14	1.3	2	18.04		33	0.42	0.91	S84
1421	-3813	0.407	-23.82	16.87	0.04	-.-	0	16.87					
1422	+2013	0.871	-24.45	17.86	0.44	-.-	0	17.86					
1424	-1150	0.806	-25.82	16.49	0.42	-.-	0	16.49					
1425	+2645	0.366	-25.05	15.68	0.20	1.0	3	16.05		25,19a	2.20	0.27	S84
1433	+1742	1.203	-24.78	18.20	0.32	-.-	0	18.20					
1451	-3735	0.314	-23.76	16.69	0.09	-.-	0	16.69			1.5	0.2	IT90
1453	-1056	0.938	-25.02	17.37	0.44	-.-	0	17.37			1.64	0.54	MS84
1454	-0605	1.249	-25.29	18.03	0.36	-.-	0	18.03					
1458	+7152	0.905	-25.66	16.78	0.46	0.2	2	16.78		40	1.41	0.60	S84,I91,W92
1502	+0338	0.411	-23.36	18.72	0.47	-.-	0	18.72					
1508	-0531	1.191	-25.43	17.21	0.23	-.-	0	17.21			1.51	0.46	S84
1509	+1551	0.828	-24.89	18.20	0.66	-.-	0	18.20					
1510	-0854	0.361	-24.08	16.54	0.20	1.5	3	17.00	2	42	1.90	0.40	IT90,W92
1511	+1022	1.546	-25.11	18.13	0.03	-.-	0	18.13			0.58	0.50	S84
1512	+3701	0.370	-24.13	16.27	-.02	-.-	0	16.27			1.10	0.23	S84
1525	+2243	0.253	-23.11	16.72	0.07	-.-	0	16.72			0.63	0.32	S84
1530	+1342	0.771	-23.07	18.99	0.33	-.-	0	18.99					
1545	+2101	0.264	-23.39	16.69	0.11	1.8	3	16.69		4,6	1.03	0.20	S84
1546	+0246	0.413	-23.32	17.79	0.17	-.-	0	17.79					
1547	+1844	1.442	-23.66	20.13	0.34	1.4	1	20.13		48			
1548	+1129	0.436	-24.11	17.23	0.24	-.-	0	17.23			0.87	1.31	S84
1551	+1305	1.290	-25.95	17.65	0.40	-.-	0	17.65			0.72	0.95	W92
1602	-0011	1.625	-25.95	17.14	0.15	0.3	1	17.49		48			
1615	+0254	1.339	-25.26	17.81	-.04	-.-	0	17.81					
1617	+1731	0.114	-22.30	15.46	0.17	2.1	3	15.80	2	37	0.94	0.17	B90
1618	+1743	0.555	-23.71	16.41	0.12	1.1	3	17.40	2	42	0.81	0.42	S84
1622	+2352	0.927	-24.91	17.47	0.44	1.2	2	17.47		33			
1634	+2654	0.561	-23.83	17.75	0.26	-.-	0	17.75					
1641	+3954	0.594	-24.55	15.96	0.29	2.6	3	17.20	2	41,42	4.00	0.30	IT90
1656	+0519	0.879	-25.05	16.54	0.46	0.8	1	17.34		32	3.34	0.61	IT90,W92
1704	+6048	0.371	-24.79	15.28	0.13	1.2	3	16.10	2	3,8,42	0.31	0.17	S84
1725	+0429	0.296	-24.48	16.99	0.44	-.-	0	16.99					
1749	+0939	0.320	-25.65	16.78	0.68	-.-	0	16.78			6.0	1.8	IT90
1821	+1042	1.360	-26.48	17.27	0.39	-.-	0	17.27					
1828	+4842	0.692	-24.78	16.81	0.24	0.6	3	17.10	2	8,40	1.19	0.48	S84,W92
1830	+2831	0.594	-24.03	17.16	-.25	-.-	0	17.16			1.28	0.56	S84
1912	-5500	0.398	-24.35	16.49	0.09	-.-	0	16.49					
1914	-4535	0.364	-24.32	16.80	0.21	-.-	0	16.80					
1942	-5707	0.527	-24.60	16.93	0.25	-.-	0	16.93					
1954	-3853	0.626	-25.84	17.07	0.61	0.8	2	17.07		2,18	10.9	0.3	IT90
2020	-3705	1.048	-24.90	17.50	0.33	0.3	2	17.50		17			
2058	-4231	0.221	-22.96	17.20	0.36	-.-	0	17.20					
2059	+0329	1.013	-24.48	17.78	0.35	1.0	3	17.80	2	42	1.73	0.72	W92
2115	-3031	0.980	-25.23	16.47	0.49	1.0	2	17.40	2	2,18			
2124	-1204	0.873	-22.56	19.35	0.22	-.-	0	19.35					
2128	-1220	0.501	-24.95	15.98	0.13	1.1	3	16.20	4	42,32	0.56	0.19	S84
2128	+0859	0.986	-24.45	18.49	0.58	-.-	0	18.49					
2135	-1446	0.200	-22.89	15.53	0.10	1.6	3	16.10	2	5,42	0.34	0.34	S84
2141	+1730	0.213	-23.67	15.73	0.18	-.-	0	15.73			0.22	0.18	S84
2142	-7550	1.139	-25.91	17.30	0.49	-.-	0	17.30					

Table C.1. (continued)

RA	δ	z	M_{min}	V_{cat}	$B-V$	Δm	var	V_{min}	note	ref	P	σ_P	P-ref
2143	-1539	0.700	-25.26	17.27	0.43	-.-	0	17.27					
2144	+0915	1.113	-23.87	18.54	0.18	2.5	3	18.54	4	2,42			
2145	+0643	0.990	-25.92	16.47	0.41	1.0	3	16.47	4	37	1.03	0.38	W92
2153	-2026	1.309	-25.86	17.01	0.14	-.-	0	17.01					
2201	+3131	0.298	-25.36	15.97	0.39	0.5	2	15.97		32,44	0.23	0.14	S84,W92
2216	-0350	0.901	-26.04	16.38	0.55	0.7	3	16.70	2	8	1.09	0.44	S84,W92
2223	-0512	1.404	-25.43	18.39	0.44	3.4	3	18.60	2	47	13.6	0.40	IT90,W92
2230	+1128	1.037	-24.83	17.33	0.42	1.1	3	17.80	2	8,42	7.3	0.30	IT90
2243	-1222	0.630	-25.06	16.45	0.18	0.5	1	16.45		21	3.3	0.4	IT90,W92
2247	+1403	0.237	-23.10	16.93	0.22	-.-	0	16.93			1.39	0.38	S84
2251	+1552	0.859	-25.29	16.10	0.47	2.4	3	17.10	2	42	2.90	0.30	IT90,W92
2251	+1120	0.323	-24.81	15.82	0.21	0.4	3	16.10	2	2,5,36	1.00	0.15	S84
2255	-2814	0.926	-26.09	16.77	0.58	-.-	0	16.77			2.00	0.40	IT90
2300	-6823	0.512	-25.06	16.38	0.22	-.-	0	16.38					
2302	-7119	0.384	-22.92	17.50	-.10	-.-	0	17.50					
2305	+1845	0.313	-23.08	17.50	0.13	-.-	0	17.50			0.38	0.45	S84
2308	+0951	0.432	-25.05	16.00	0.15	-.-	0	16.00			1.14	0.16	S84
2314	+0348	0.220	-24.23	17.54	0.86	-.-	0	17.54					
2325	+2920	1.015	-25.96	17.30	0.65	-.-	0	17.30					
2326	-4746	1.299	-26.35	16.79	0.25	-.-	0	16.79			1.0	0.30	IT90
2329	-3828	1.195	-25.87	17.04	0.31	-.-	0	17.04					
2335	-1808	1.441	-25.78	17.34	0.07	1.7	3	17.34	4	42			
2340	-0340	0.896	-26.58	16.05	0.52	-.-	0	16.05			0.87	0.25	S84
2344	+0914	0.677	-25.83	15.97	0.23	0.3	3	15.97		27,43	0.90	0.34	S84
2345	-1647	0.576	-23.34	18.41	0.30	2.8	3	18.41	4!	42	4.90	1.50	IT90
2349	-0125	0.173	-22.66	15.33	0.12	1.6	3	16.00	2	42	0.91	0.21	S84

Notes:
1 – averages for $B-V$ and/or V
2 – V_{min} estimated from photographic light-curve in B or from ITS counts
3 – V_{min} originally estimated from the PSA
4 – Δm from $\mid V_{cat} - V_{lightcurve} \mid$ (4! problematic)

References for variability: 1. Adam (1978) 2. Adam (1985) 3. Angione (1971) 4. Angione (1973) 5. Angione et al. (1981) 6. Barbieri & Romano (1981) 7. Barbieri et al (1967) 8. Barbieri et al (1978) 9. Barbieri et al. (1979) 10. Bolton et al. (1966) 11. Browne et al (1975) 12. Cutri et al. (1985) 13. Downes et al (1986) 14. Eggen (1973) 15. Ellingson et al. (1989) 16. Folsom et al. (1971) 17. Gilmore (1979) 18. Gilmore (1980) 19. Grandi & Tifft (1974) 19a. Greenstein & Oke (1970) 20. Hunter & Lü (1969) 21. Impey & Tapia (1988) 22. Jackish (1971) 23. Jauncey et al. (1978) 24. Kinman (1976) 24a. Kinnander (1981) 25. Lloyd (1984) 26. Lynds & Wills (1972) 27. Lü (1972) 28. McGimsey et al. (1975) 29. Miller (1977) 30. Miller (1980) 31. Mullikin & Miller (1977) 32. Moles et al. (1985) 33. Moore & Stockman (1984) 34. Peach (1969) 35. Peterson & Bolton (1972) 36. Pica & Smith (1983) 37. Pica et al. (1980) 38. Sandage (1966) 39. Sandage et al. (1965) 40. Selmes et al. (1975) 41. Sillanpää et al. (1988) 42. Smith et al. (1993) 43. Tritton & Selmes (1971) 44. Tritton et al. (1973) 45. Uomoto et al. (1976) 46. Usher (1978) 47. Webb et al. (1988) 48. Wills & Lynds (1978)

References for polarization: S84 = Stockman et al. 1984, MS84 = Moore & Stockman 1984, B90 = Berriman et al. 1990, IT90 = Impey & Tapia 1990, W92 = Wills et al. 1992, BT99 = Berdyugin & Teerikorpi (in preparation)

where the right side with $E(B-V)=1$ will be denoted by $S(\lambda)$ in what follows. With the $1/\lambda$-dependence, S becomes $S(\lambda)=\lambda_V R_V/\lambda - R_V$.

In the intervening galaxy, where the extinction takes place, the dust sees the radiation which eventually falls on our V-band, at $\lambda_{V\,obs}=\lambda_V/(1+z)$. Hence the extinction suffered by the light is given by $E(V_{obs}-V)=E(B-V)S(\lambda/(1+z))$, where V and $B-V$ are for the astronomer on that galaxy the same bands as we use. $E(V_{obs})=E(V_{obs}-V)+A_V$, where A_V is the extinction at the V-band at z, or

$$E(V_{obs})=S(\lambda_V/(1+z))E(B-V)+A_V$$

It is a delightful property of the $1/\lambda$-extinction curve that the above expression is simplified into

$$E(V_{obs})=A_V(1+z)$$

and $R_V=E(V_{obs})/E(B_{obs}-V_{obs})$ *does not depend on the redshift of the dust*. Both the observed $B-V$-reddening and the V-extinction are increased by the same factor $1+z$. Though the $1/\lambda$-law is not exactly valid everywhere, the above result is a quick approximation. That R_V does not depend on $z(dust)$ facilitates the use of $B-V$ as an extinction indicator, independently of where the dust is.

Appendix C: data for the basic sample

The basic data are given in Table C1:

1,2) coordinates α, δ
3) redshift z,
4) absolute minimum brightness V magnitude, M_{min}
5) catalog V magnitude, V_{cat}
6) colour $B-V$,
7) variability amplitude Δm,
8) variability information level: 0 (none) - 3 (good),
9) notes about magnitudes and variability amplitudes,
10) references for variability,
11) optical polarization P (percent),
12) standard error of polarization σ_P,
13) references for polarization.

References

Adam G., 1978, A&AS 31, 151
Adam G., 1985, A&AS 61, 225
Angione R.J., 1971, AJ 76, 25
Angione R.J., 1973 AJ 78, 353
Angione R.J., Moore E.P., Roosen R.G., Sievers J., 1981, AJ 86, 653
Bahcall J.N., Kirhakos S., Schneider D.P., 1995, ApJ 450, 486
Barbieri C., Battistini P., Nasi E., 1967, Publ. Oss. Padova No. 141
Barbieri C., Romano G., Zambon M., 1978, A&AS 31, 401
Barbieri C., Romano G., Zambon M., 1979, A&AS 37, 551
Barbieri C., Romano G., 1981, A&AS 44, 159
Berdyugin A., Snåre M.-O., Teerikorpi P., 1995, A&A 294, 568
Berdyugin A., Teerikorpi P., 1997, A&A 318, 37
Berriman G., Schmidt G.D., West S.C., Stockman H.S., 1990, ApJSS 74, 869
Bolton J.G., Shimmins A.J., Ekers J., et al., 1966, ApJ 144, 1229
Browne I.W.A., Savage A., Bolton J.G., 1975 MNRAS 173, 87P
Cristiani S., Vio R., 1990, A&A 227, 385
Cristiani S., Trentini S., La Franca F., et al., 1996, A&A 306, 395
Cutri R.M., Wisniewski W.Z., Rieke G.H., Lebofsky M.J., 1985, ApJ 296, 423
Downes A.J.B., Peacock J.A., Savage A., Carrie D.R., 1986, MNRAS 218, 31
Eggen O.J., 1973, ApJ 186, L1
Ellingson E., Yee H.K.C., Green R.F., Kinman T.D., 1989, AJ 97, 1539
Fabian A.C., Crawford C.S., 1990, MNRAS 247, 439
Folsom G.M., Smith A.G., Hackney R.L., Hackney K.R., 1971, Nat. Phys. Sci. 230, 199
Giallongo E., Trevese D., Vagnetti F., 1991, ApJ 377, 345
Gilmore G., 1979, MNRAS 187, 389
Gilmore G., 1980, MNRAS 190, 649
Grandi S.A., Tifft W.G., 1974, PASP 86, 873
Greenstein J.L., Oke J.B., 1970, PASP 82, 898
Haarala S., Teerikorpi P., 1986, Ap&SS 122, 163
Hewitt A., Burbidge G., 1993, ApJS 87, 451
Hintz E.G., Roming P.W.A., Moody J.W., Miller K.A., 1997, AJ 113, 1375
Hook I.M., McMahon R.G., Boyle B.J., Irwin M.J., 1994, MNRAS 268, 305
Hunter J.H., Lü P.K., 1969, Nat 223, 1045
Hutsemekers D., 1998, A&A 332, 410
Impey C.D., Tapia S., 1988, ApJ 333, 666
Impey C.D., Tapia S., 1990, ApJ 354, 124
Impey C.D., Lawrence C.R., Tapia S., 1991, ApJ 375, 46
Jackisch G., 1971, Astron. Nachr. 292, 271
Jauncey D.L., Wright A.E., Peterson B.A., Condon J.J., 1978, ApJ 219, L1
Kinman T.D., 1976, ApJ 205, 1
Kinnander A., 1981, A&A 99, 63
Komberg B.V., 1982, Preprint 727, Institute of Cosmic Research
Komberg B.V., 1984, Astrofizika 20, 73
Kormendy J., Richstone D., 1995, ARA&A 33, 581
Kotilainen J., Falomo R., Scarpa R., 1998, A&A 332, 503
La Franca F., Gregorini L., Cristiani S., De Ruiter H., Owen F., 1994, AJ 108, 1548
Lloyd C., 1984, MNRAS 209, 697
Lynds R., Wills D., 1972, ApJ 172, 531
Lü P.K., 1972, AJ 77, 829
Mack C., 1975, Essentials of Statistics for Scientists and Technologists. Plenum Press, New York
Magorrian J., Tremaine S., Richstone D., et al., 1998, AJ 115, 2285
Malkan M.A., 1983, ApJ 268, 582
Mattig W., 1958, Astron. Nachr. 284, 109
McGimsey B.Q., Smith A.G., Scott R.L., et al. 1975, AJ 80, 895
Miller H.R., 1977, A&A 54, 537
Miller H.R., 1980, AJ 85, 99
Moles M., Garcia-Pelayo J.M., Masegosa J, et al., 1985, A&A 152, 271
Moore R.L., Stockman H.S., 1984, ApJ 279, 465
Mullikin T.L., Miller H.R., 1977, PASP 89, 639
Ostriker J.P., Heisler J., 1984, ApJ 278, 1
Peach J.V., 1969, Nat 222, 439
Peterson B.A., Bolton J.G., 1972, Astrophys. Letters 10, 105
Pica A.J., Smith A.G., 1983, ApJ 272, 11
Pica A.J., Pollock J.T., Smith A.G., et al., 1980 AJ 85, 1442
Sandage A., 1966, ApJ 144, 1234
Sandage A., Véron P., Wyndham J.D., 1965, ApJ 142, 1307
Savage B.D., Mathis J.S., 1979, ARA&A 17, 73
Scott R.L., Leacock R.J., McGimsey B.Q., et al., 1976, AJ 81, 7
Selmes R.A., Tritton K.P., Wordsworth R.W., 1975, MNRAS 170, 15
Sillanpää A., Haarala S., Korhonen T., 1988, A&AS 72, 347
Simmons J.F.L., Stewart B.G., 1985, A&A 142, 100
Smith A.G., Nair A.D., Leacock R.J., Clements S.D., 1993, AJ 105, 437
Stockman H.S., Moore R.L., Angel J.R.P., 1984, ApJ 279, 485
Teerikorpi P., 1978, A&A 64, 379
Teerikorpi P., 1981a, A&A 98, 300 (Paper Ia)
Teerikorpi P., 1981b, A&A 98, 309 (Paper I)
Teerikorpi P., 1990, A&A 235, 362
Teerikorpi P., 1997, ARA&A 35, 101
Teerikorpi P., 1998, A&A 339, 647 (T98)
Teerikorpi P., Kotilainen J., 1989, Ap&SS 155, 19
Tritton K.P., Selmes R.A., 1971, MNRAS 153, 453
Tritton K.P., Henbest S.N., Penston M.V., 1973, MNRAS 162, 31P
Uomoto A.K., Wills B.J., Wills D., 1976, AJ 81, 905
Usher P.D., 1978, ApJ 222, 40
Véron P., Hawkins M.R.S., 1995, A&A 296, 665
Véron-Cetty M.-P., Véron P., 1993, Scientific Report No. 13, ESO
Webb J.R., Smith A.G., Leacock R.J., et al., 1988, AJ 95, 374
Wills D., Lynds R., 1978, ApJS 36, 317
Wills B.J., Wills D., Breger M., Antonucci R.R.J., Barvainis R., 1992, ApJ 398, 454
Wilson A.S., Colbert E.J.M., 1995, ApJ 438, 62
Wisotzky L., 1998, Astron. Nachr. 391, 257
Yee H.K.C., Green R.F., 1987, ApJ 319, 28